Physical Properties of Natural Rubber/Organoclay Nanocomposites Compatibilized with Epoxidized Natural Rubber

P. L. Teh,[1] Z. A. Mohd Ishak,[1] A. S. Hashim,[1] J. Karger-Kocsis,[2] U. S. Ishiaku[3]

[1]*School of Materials and Mineral Resources Engineering, Engineering Campus, Universiti Sains Malaysia, Penang, Malaysia*
[2]*Institut für Verbundwerkstoffe GmbH, (Institute for Composite Materials) Kaiserslautern University of Technology, D-67653 Kaiserslautern, Germany*
[3]*Advanced Fibro-Science, Kyoto Institute of Technology, Matsugasaki, Sakyo-ku, Kyoto 606-8585, Japan*

Received 15 January 2004; accepted 30 August 2005
DOI 10.1002/app.23452
Published online in Wiley InterScience (www.interscience.wiley.com).

ABSTRACT: Onium ion-modified montmorillonite (organoclay) was melt compounded with natural rubber (NR) in an internal mixer and cured by using a conventional sulfuric system. Epoxidized natural rubber with 50 mol % epoxidation (ENR 50) was used in 10 parts per hundred rubber (phr) as a compatibilizer. The effect of organoclay with different filler loading up to 10 phr was studied. Cure characteristics were determined by a Monsanto MDR2000 rheometer, whereas the tensile, compression, and tear properties of the nanocomposites were measured according to the related ASTM standards. While the torque maximum and torque minimum increased slightly, both scorch time and cure time reduced with the incorporation of organoclay. The tensile strength, elongation at break, and tear properties went through a maximum (at about 2 phr) as a function of the organoclay content. As expected, the hardness, moduli at 100% (M100) and 300% elongations (M300) increased continuously with increasing organoclay loading. The compression set decreased with incorporation of organoclay. The dispersion of the organoclay in the NR stocks was investigated by X-ray diffraction and transmission electron microscopy. © 2006 Wiley Periodicals, Inc. J Appl Polym Sci 100: 1083–1092, 2006

Key words: natural rubber (NR); organoclay; nanocomposite; epoxidized natural rubber (ENR)

INTRODUCTION

Reinforcement of polymer with nano-sized particles is a promising technique that is capable of yielding materials with enhanced performance without involvement in expensive synthesis procedures. A very small fraction (i.e., a few weight percent) of the silicate filler would give significant improvements in the stiffness and strength of the related materials.[1,2]

Polymer/clay nanocomposites are being investigated and developed worldwide by a number of public, private, and corporate entities. The nanocomposites can be grouped according to their matrices: (a) thermoplastics, (b) thermosets, and (c) rubbers. Recently, the R and D activity on polymer–organoclay nanocomposites was focused on thermoplastic matrices, such as polyamide, polypropylene, poly(methyl methacrylate), and polystyrene.[3–8] Extensive research has been done also on thermosetting systems.[9–11] Tremendous improvements in mechanical properties, enhancement of heat stability, abrasion resistance, solvent resistance, reduced gas permeability, and improved flame retardancy have been achieved by optimizing the interactions between the reinforcing layered silicate and matrix, which resulted in a nanoscale dispersion of the silicate.[12]

Up to now, only few studies were devoted to rubber-based nanocomposites. In case of rubber stocks, the biggest challenge is to find alternative white fillers to replace carbon black and silica. Usually, the optimum level of organoclay loading is below 10 parts per hundred rubber (phr). Mousa et al.[13] found that 10 phr of organoclay improved the viscoelastics and tensile behavior of styrene/butadiene-based rubber vulcanizates. Nah et al.[14] showed that only 15 phr of organoclay was necessary to obtain optimum tensile and tear properties, which were comparable to a compound loaded with 40 phr carbon black.

To render the pristine clay (hydrophilic) compatible with the polymer (hydrophobic), the clay has to be modified accordingly. Polymer compatible organophilic clays (organoclays) are made by intercalation with organic cations exploiting the cation exchange

Correspondence to: Z. A. Mohd Ishak (zarifin@eng.usm.my).

Contract grant sponsor: Ministry of Science, Technology, and Environment (MOSTE), Malaysia; contract grant number: 063171/IRPA.

TABLE I
Composition of the Rubber Compounding

Ingredient	Content (phr)[a]
Natural rubber (SMR L)	100
ENR 50	10
Organoclay (MMT)	0,2,4,6,8,10
Sulphur	2.5
Zinc oxide	5.0
IPPD	2.0
Stearic acid	1.0
CBS	0.5

ENR, epoxidized natural rubber; IPPD, *N*-isopropyl-*N*-phenyl-*p*-phenylenediamine; CBS, *N*-cyclohexyl-2-benzothiazyl sulphenamide.

[a] Parts per hundred parts of rubber.

capacity of some layered clays. Exchange of the alkali cations by long alkyl chained amines and ammonium compounds (onium intercalation) opens the distance between the clay platelets (layers, galleries), which becomes thus accessible for the polymer chains.[2,15]

Nano-sized filled composites can be considered as the latest development in advanced materials technology. Since natural rubber (NR) does not have polar groups in its backbone, it was the aim of this study to investigate the role of a functionalized NR, *viz*. epoxidized natural rubber (ENR), in respect with the curing and properties of the NR/ENR/organoclay nanocomposites.

EXPERIMENTAL

Materials

The elastomers used were NR (SMR L) and ENR with the Mooney viscosity of ML (1 + 4) 100°C = 78, ML (1 + 4) = 140, respectively, both purchased from Kumpulan Guthrie Sdn. Bhd., Seremban, Malaysia. The ENR contained 50 mol % epoxidation (denoted further as ENR 50). Montmorillonite modified with octadecyltrimethylammonium salt (Nanomer I.28E) supplied by Nanocor Inc., USA was used in this study. Other compounding ingredients such as sulfur, zinc oxide, stearic acid, *N*-isopropyl-*N*′-phenyl-*p*-phenylenediamine (IPPD), *N*-cyclohexyl-2-benzothiazyl sulfenamide were purchased from Bayer (M) Sdn. Bhd, Malaysia.

Compounding

A conventional vulcanization system was used for compounding. Table I shows the composition of the rubber stocks. The master batch (MB) preparation was done by using a Banbury internal mixer model BR1600. The rubber was masticated for half minute and all ingredients, except curatives, were added and mixing continued for another two and a half minutes. The compounding was done at 80°C and 100 rpm for 3 min. Curatives were mixed into MB by using a two-roll mill sized (160 × 320 mm^2), according to ASTM designation D 3184–80 at 70 ± 5°C for 2 min.

Cure characterization

Compound cure characteristics were measured using a Monsanto Moving Die Rheometer, model MDR 2000, at 150°C, according to ASTM 2240–93.

Compression molding

The vulcanizates were prepared by curing the rubber sheets under pressure (10 MPa) at 150°C in a KAO Tech hot press for the respective cure times, t_{90} determined from the MDR 2000 tests. Vulcanized sheets of 2 mm thickness were produced.

Tensile properties

Dumbbell-shaped samples were cut from the molded sheets, according to ASTM D412–93. Tensile properties were determined on a Monsanto Tensometer M500 with the crosshead speed of 500 mm/min.

Tear properties

Crescent-shaped samples type die B were stamp from the molded sheets, according to ASTM D624–9. A nick (0.50 ± 0.05 mm) in depth was produced by using a sharp razor blade. Tear strength was determined on a Monsanto Tensometer M500 with the crosshead speed of 500 mm/min.

Hardness

The hardness of the rubber vulcanizates were carried out according to ASTM D2240, with international rubber hardness tester. Specimens with the thickness of 6 mm will be obtained from molding. The test will be carried out at room temperature. The value will be reported based on the average of five measurements.

Compression set

Specimens used for this test were disc pieces 12.5 ± 0.5 mm in thickness, according to ASTM D395, method B. Compression device consists of two or three flat steel plates between the parallel faces of which the specimens may be compressed. Steel spacers for the required percentage of compression employed were ~25% for all hardness. The spacers have a thickness of 9.5 ± 0.2 mm.

The original thickness of specimen was measured to nearest 0.02 mm and the specimens were placed between the plates of compression device with spacers

on each side. The bolts were tightened so that the plates were drawn together uniformly until they were in contact with the spacers. The assembled compression device was subjected to testing temperature (70°C) for 22 h. At the end of the period, the test specimen was removed immediately and after 30 min, the final thickness at the center of the test specimen was measured.

The compression set, C, expressed as a percentage of the original deflection was calculated as follows:

$$C(\%) = (t_0 - t_1)/(t_0 - t_n) \times 100 \quad (1)$$

Where t_o is the original thickness of specimen; t_1 the final thickness of specimen; and t_n the thickness of the spacer.

Scanning electron microscopy (SEM)

The facture surface of the vulcanizates was studied with a Leica Cambridge S-360 scanning electron microscope. The fracture surfaces were coated by gold to prevent electrostatic charging during examination.

Dynamic mechanical thermal analysis (DMTA)

The complex modulus (E^*), its storage (E') and loss parts (E″), and the mechanical loss factor (tan $\delta = E''/E'$), as a function of temperature (T), were assessed by DMTA using an Eplexor 25N device of Gabo Qualimeter, Germany. DMTA spectra were taken in tension mode at a frequency of 10 Hz in a broad temperature range ($T = -100$ to $+100$°C). The DMTA device operated under load control.

X-ray diffraction (XRD)

Wide-angle X-ray spectra were recorded with a D 500 diffractometer (Siemens, Germany) in step scan mode using Ni-filtered Cu Kα radiation (0.1542 nm wavelength). Powder samples were scanned in reflection, whereas the molded compounds in transmission in the interval of $2\theta = 1°$–$12°$. The interlayer spacing, d-spacing of the organoclay, was derived from the peak position (d_{001}-reflection) in the XRD diffractograms, according to the Bragg equation[16]:

$$\lambda = 2d \sin\theta \quad (2)$$

Where λ is the X-ray wavelength, d is the interlayer spacing, and θ is the angle of diffraction.

Transmission electron microscopy (TEM)

TEM measurements were carried out with a LEO 912 Omega transmission electron microscope by applying an acceleration voltage of 120 keV. The specimens were prepared using an Ultracut E (Reichert and Jung) ultramicrotome. Thin sections of about 100 nm thickness were cut with a diamond knife at about −100°C.

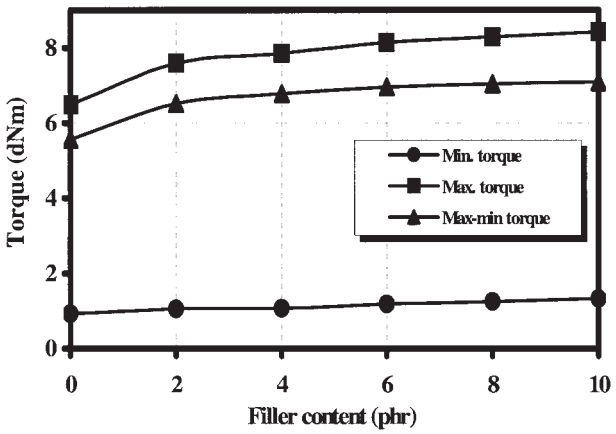

Figure 1 Torque maximum (M_H), torque minimum (M_L), and the torque difference (M_H–M_L) for NR/ENR 50/organoclay nanocomposites at varying filler contents.

RESULTS AND DISCUSSION

Cure characterization

Figure 1 shows the effect of organoclay loading on the cure characteristic of NR/ENR 50/organoclay nanocomposites. Torque minimum (M_L) increases slightly with increase in filler loading. Since the torque minimum can be regarded a measure of the stock viscosity, this implies that incorporation of organoclay increases the viscosity of the nanocomposites. This perhaps may be explained with the Einstein, Guth, and Gold equation[17]:

$$\eta_f = \eta_u(1 + 2.5c + 14.1c^2) \quad (3)$$

Where the η_f and η_u are the viscosities of the filled and unfilled nanocomposite, and c is the volume fraction of the fillers. From eq. (3), it is obvious that the viscosity is expected to increase with increase in filler loading. However, the increases of viscosity could also be affected by the agglomeration of the organoclay in the rubber matrix.

In Figure 1, the torque maximum (M_H) increases with increasing organoclay loading. The torque maximum is correlated with durometer modulus and hardness.[18] Since the modulus of organoclay is higher than rubber matrix, the incorporation of organoclay will increase the stiffness of the nanocomposite. A similar trend observed for torque difference (M_H–M_L) (shown in Fig. 1) indicates the extent of crosslinking and rubber-filler interaction of the nanocomposite. M_H–M_L is a measure of the shear dynamic modulus,

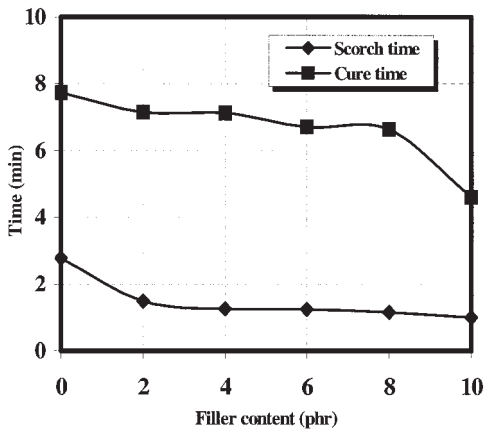

Figure 2 Cure (t_{90}) and scorch times (t_2) for NR/ENR 50/organoclay nanocomposites at varying filler contents.

which indirectly relates to the crosslink density of the nanocomposites.[19]

Figure 2 shows the scorch time (t_2) and cure time (t_{90}) of the NR/ENR 50/organoclay nanocomposites. It can be seen that the t_2 and t_{90} of the nanocomposites reduce gradually with organoclay addition. This may be attributed to the presence of the amine functional groups in the organoclay (as a result of the ion exchange process). Recall that amine containing compounds usually facilitate the curing reaction of NR stocks.[13]

Table II shows the scorch time (t_{90}), maximum torque (M_H), minimum torque (M_L), and max–min torque (M_H–M_L) of NR nanocomposites filled with 2 phr of organoclay with and without ENR 50 compatibilizer. Note that ENR 50 reduced both the t_{90} and scorch time values. This is due to the activation of an adjacent double bond by the epoxide group in the ENR 50 compatibilized stock.[20]

NR/ENR 50/organoclay also displays a higher maximum torque as compared to NR/organoclay. As maximum torque is correlated with durometer modulus and hardness,[18] this indicates that incorporation of ENR 50 has increased the stiffness of the NR/ENR 50/organoclay nanocomposite. The lower value of minimum torque of NR/ENR 50/organoclay indicates that ENR 50 has improved the processability of the nanocomposite. The higher torque difference (M_H–M_L) of NR/ENR50/organoclay provide a good indication of the higher extent of crosslinking of the nanocomposites.[19]

Tensile properties

The effect of the organoclay loading on the tensile properties of the NR/ENR 50/organoclay nanocomposites is shown in Figure 3. The tensile strength increases to a plateau at 2 phr, which ends at about 6 phr organoclay loading. It is believed that up to 2 phr filler loading, the organoclay is uniformly dispersed (i.e., well intercalated and exfoliated) in the NR matrix. This will be supported by the TEM study reported later. The organoclay platelets possess an extremely high aspect ratio [21] and thus act as reinforcing elements, assuming a good filler-rubber interaction. The amine intercalant octadecyltrimethylamine of the organoclay, which may react with the epoxide groups of the ENR 50, likely facilitate the disintegration of the layered clay particles. The resulting intercalation/exfoliation should improve the interfacial bonding between the rubber and clay layers, and as a consequence improved mechanical properties.

However, when the filler content reaches 8 phr and above, the filler tends to agglomerate. This agglomeration (shown by TEM later) leads to a reduction in the tensile characteristics.[9] The usual explanation of (re)agglomeration with increasing organoclay content is that the amount of the matrix molecules becomes less than that required for a complete exfoliation (which means an ideal intermingling between the molecules of the rubber and those of the intercalating compound of the organoclay).

The elongation at break of the nanocomposites initially remains unaffected with the incorporation of 2 phr filler content. This is believed to be related to the intercalation and exfoliation processes of the organoclay that cause higher crosslinking of the rubber in the neighborhood of the organoclay platelets.[13] As expected, further increment of filler content resulted in a gradual reduction in elongation at break. It is interesting to note that the elongation at break still remain relatively high even at 10 phr filler content. The reduction in elongation at break is believed to be caused by an increasing tendency for clay agglomeration at high filler loading.[22] This can be proven by scanning electron micrographs taken on the fracture surfaces of the rubber nanocomposite as discussed later.

Figure 4 shows the effect of organoclay loading on the tensile moduli M100 and M300 (moduli at 100 and 300% elongations, respectively), which is a measure of stiffness of rubber nanocomposites. Organoclay loading has similar effect on M100 and M300, whereby both parameters increase with increasing filler content. This was reported also for other rubber/organoclay systems.[13,23]

TABLE II
Cure Characteristic of NR Nanocomposite Filled of 2 phr Organoclay with and without ENR 50 as a Compatibilizer

Parameters	NR/ organoclay	NR/ENR 50/ organoclay
Scorch time (min)	1.62	1.49
Cure time (t_{90}) (min)	7.20	6.49
Minimum torque (M_L) (dN m)	1.44	1.33
Maximum torque (M_H) (dN m)	8.26	8.41
Max-min torque (M_H–M_L) (dN m)	6.82	7.08

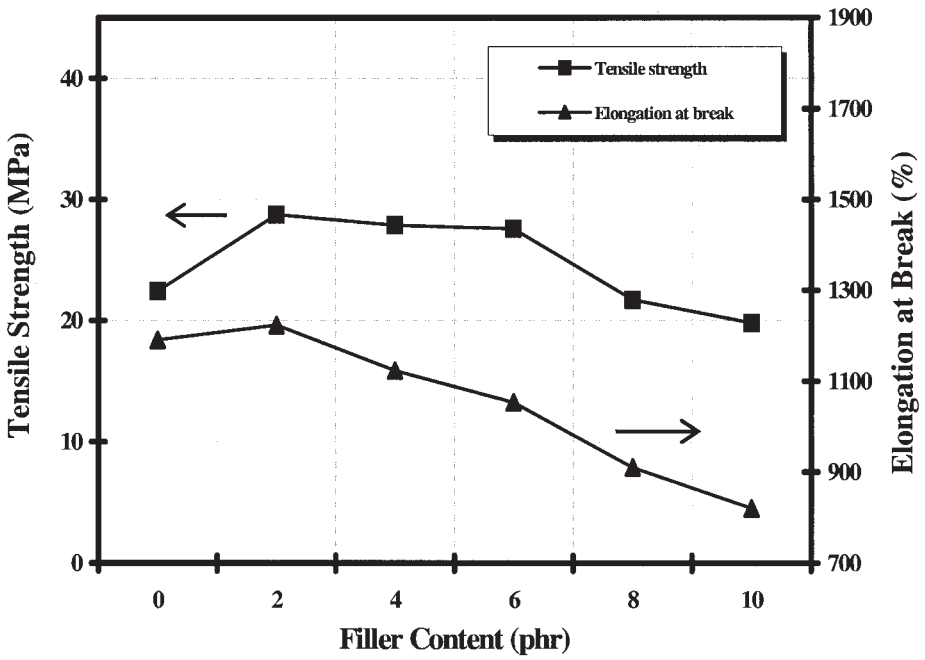

Figure 3 Effect of filler loading on the tensile strength and elongation at break of NR/ENR 50/organoclay nanocomposites.

Tear properties

The effect of organoclay loading on tear strength of NR/ENR 50/organoclay nanocomposites is shown in Figure 5. The tear strength increases gradually and remains relatively high up to 4 phr, after which it drops with further incorporation of organoclay. This trend is similar to the elongation at break (Fig. 3) to which the tear strength is related. As stated earlier, at lower filler content, the filler can be dispersed well in the rubber matrix and the extend further propagation. At higher filler content, the filler tends to form agglomerates. Such agglomerates may work as stress concentrators and thus reduce the tear strength.[22]

The effect of ENR 50 as a compatibilizer on the mechanical properties of NR nanocomposite is shown in Table III. It can be seen that incorporation of ENR 50

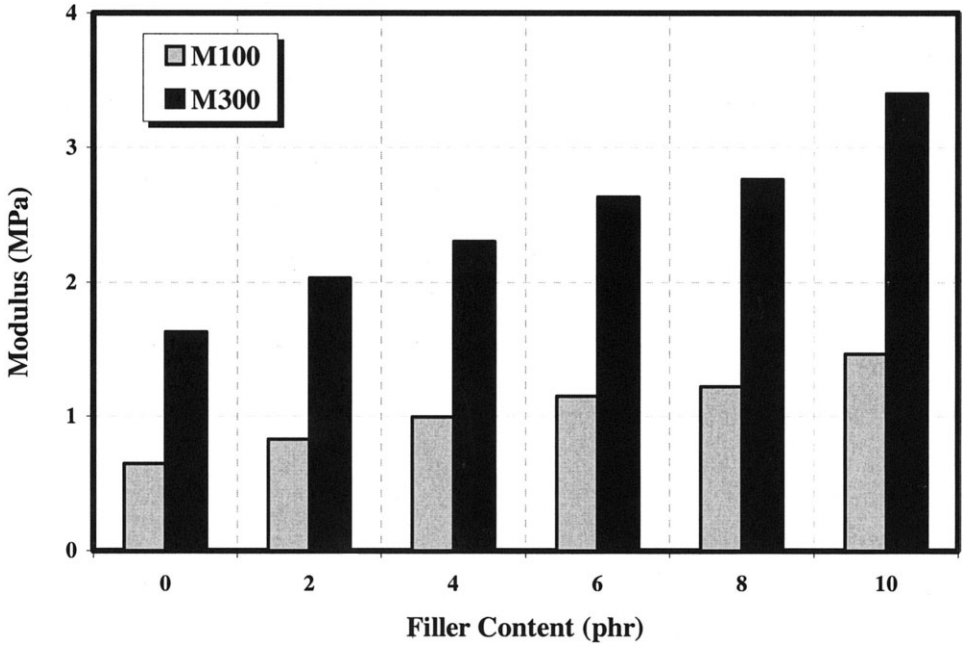

Figure 4 Effect of filler loading on the moduli at 100 and 300% elongations for the NR/ENR 50/organoclay nanocomposites.

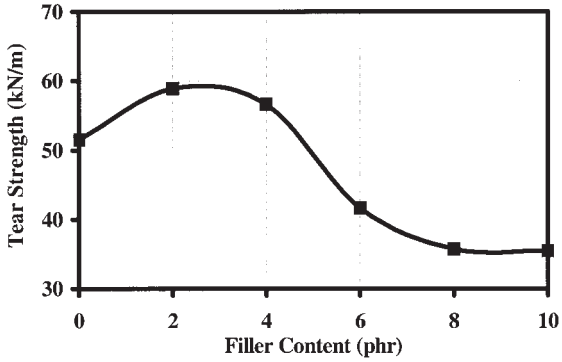

Figure 5 Effect of filler loading on the tear strength of NR/ENR 50/organoclay nanocomposites.

leads to a dramatic enhancement of mechanical properties such as tensile strength, elongation at break, modulus, and tear strength of filled NR. The enhancement of mechanical properties in the presence of the compatibilizer may be due to better organoclay dispersion.[24] This will be evident from the TEM investigations presented later.

Hardness and compression set

Figure 6 shows the results of hardness with increasing filler content. According to Brown et al., [25] hardness is essentially a measure of modulus. One can observe a very similar behavior shown in modulus measurements, i.e., a substantial increase in the value of harness as the filler content is increased.

As defined by ASTM D 1566, compression set is the residual deformation of a material after removal of the compressive stress. According to Smith [26] and Othman,[27] compression set is a measure of the ability of the rubber to retain their elastic properties after prolonged compression at a constant strain under a specified set of conditions, and it's a permanent set of rubber compounds. The compression set of filled vulcanizates shows lower value with increasing filler content, which shown in Figure 6, suggesting that the chemical structure of compound filled with 10 phr of organoclay is more stable than the others. Hao et al.[28]

TABLE III
Mechanical Properties of NR Nanocomposite Filled of 2 phr Organoclay with and without ENR 50 as a Compatibilizer

Parameter	NR/organoclay	NR/ENR 50/ organoclay
Tensile strength (MPa)	18.73	28.75
Elongation at break (%)	879.53	1223.02
M100 (MPa)	0.76	0.83
M300 (MPa)	1.93	2.03
Tear strength (kN/m)	41.75	58.89

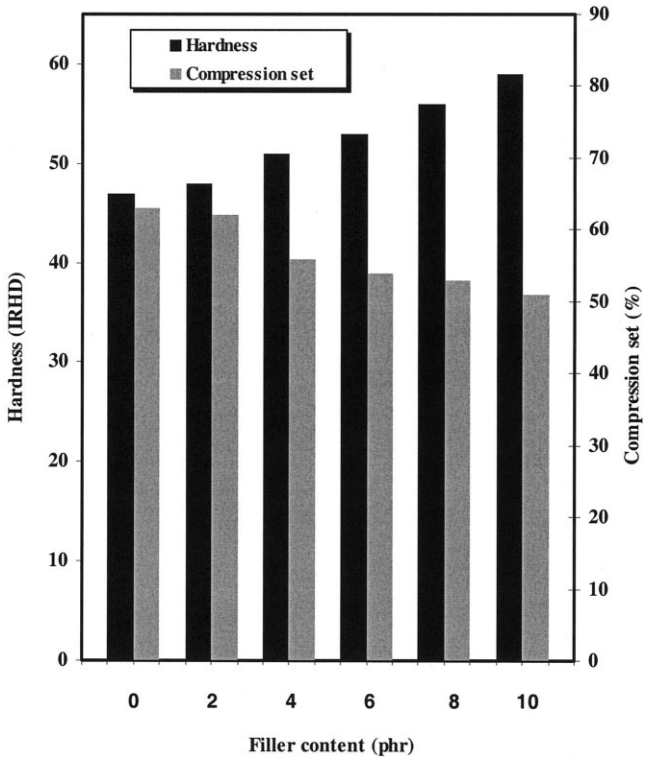

Figure 6 Effect of filler loading on the swelling index and crosslink density of NR/ENR 50/organoclay nanocomposites.

reported the increased formation of effective network chains or crosslinking in the deformed state decreases compression set.

Scanning electron microscopy

Figures 7(a)–7(c) show the tensile failure surface of the NR gum, nanocomposites filled with 2 phr, and 10 phr organoclay, respectively. The fracture surface in Figure 7(a) is fairly smooth with some tear lines. Figure 7(b) substantiates that incorporation of 2 phr organoclay strongly affected the morphology and thus also the fracture behavior. The fracture surface of this compound became rougher, which hints to the activation of additional failure mechanisms due to the presence of organoclay. Figure 7(c) shows the tensile fracture surface of the compatibilized NR with 10 phr organoclay. The formation of voids—which are absent for the 2 phr organoclay filled system [cf. Figure 7(b)]—can be attributed to the easy detachment of agglomerated particles from the matrix. Recall that this process is favored by the particle shape dependent stress concentration effects.[29] This accounts for the reduction of the tensile strength and elongation at break with increasing filler content above 2 phr organoclay content.

Dynamic mechanical thermal analysis (DMTA)

Figures 8(a) and 8(b) show the storage modulus (E'), and mechanical loss factor (tan δ) of NR/ENR 50 gum

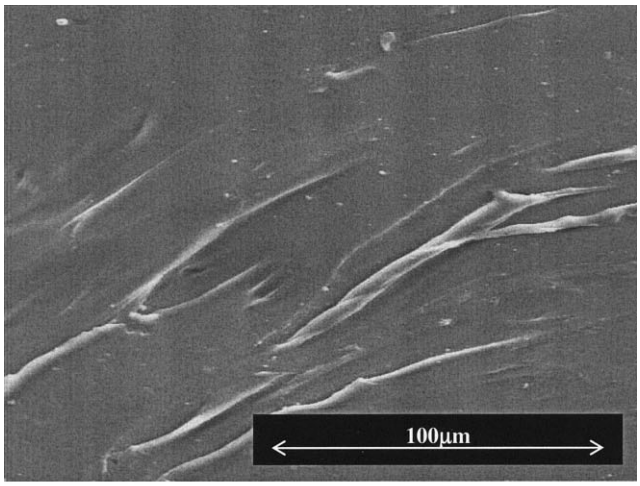

(a)

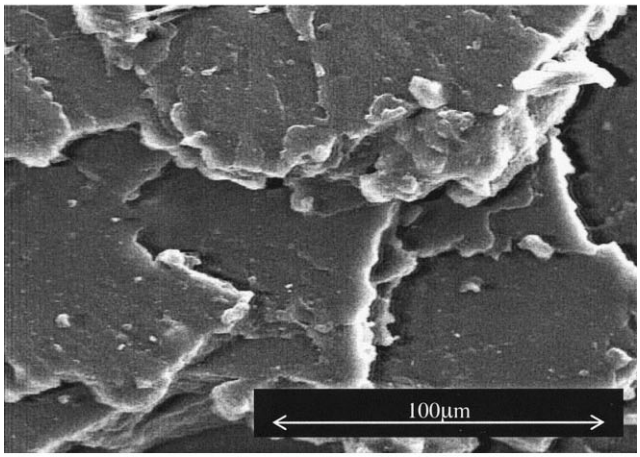

(b)

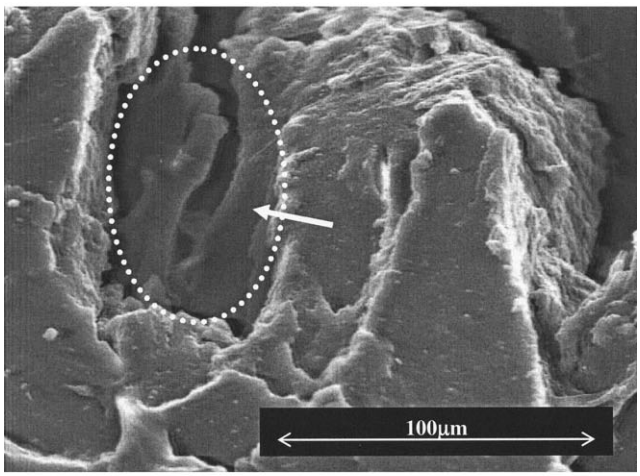

(c)

Figure 7 SEM micrograph showing tensile fracture surface of (a) the unfilled NR gum, (b) an NR/ENR 50/organoclay nanocomposite filled with 2 phr organoclay, and (c) an NR/ENR 50/organoclay nanocomposite filled with 10 phr organoclay.

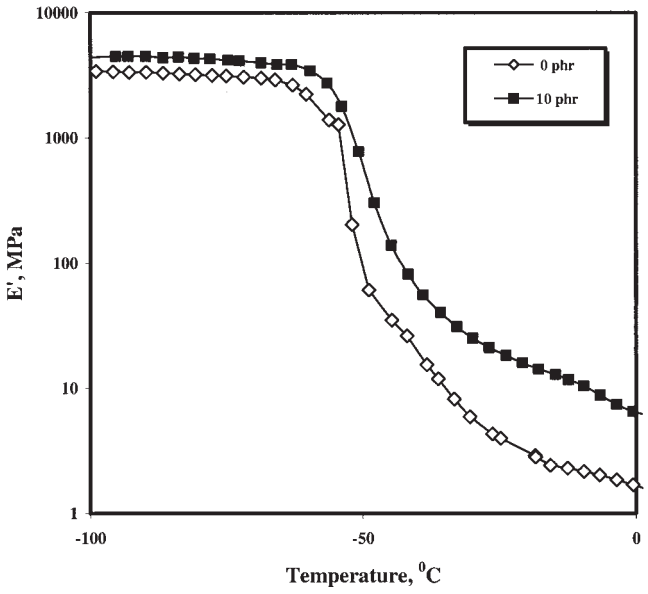

(a)

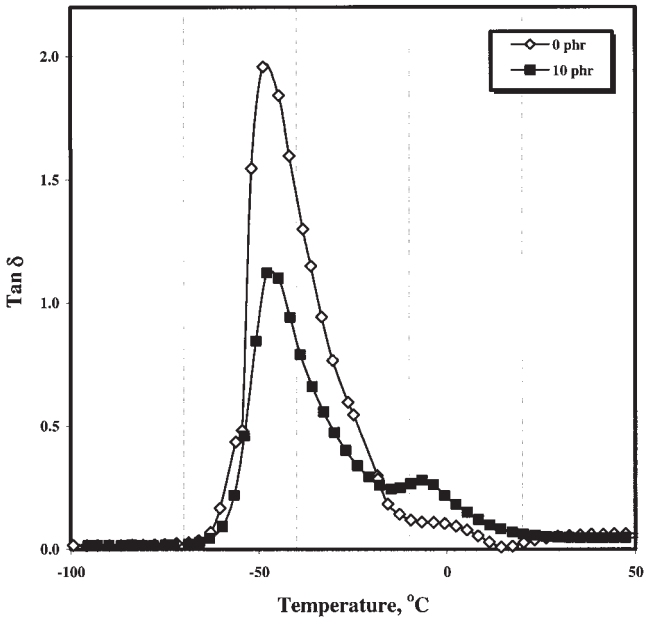

(b)

Figure 8 (a) Storage modulus (E') as a function of temperature for NR/ENR 50 gum and NR/ENR 50/organoclay nanocomposites filled with 10 phr organoclay. (b) Loss factor (tan δ) as a function of temperature for NR/ENR 50 gum and NR/ENR 50/organoclay nanocomposites filled with 10 phr organoclay.

and nanocomposite filled with 10 phr of organoclay as a function of temperature. In Figure 8(a), above glass transition region, the E' of the nanocomposite filled with 10 phr organoclay shows a higher value than the reference compound. This shows that the addition of organoclay into the NR/ENR 50 blend results in a remarkable increase of stiffness. Note that this is the

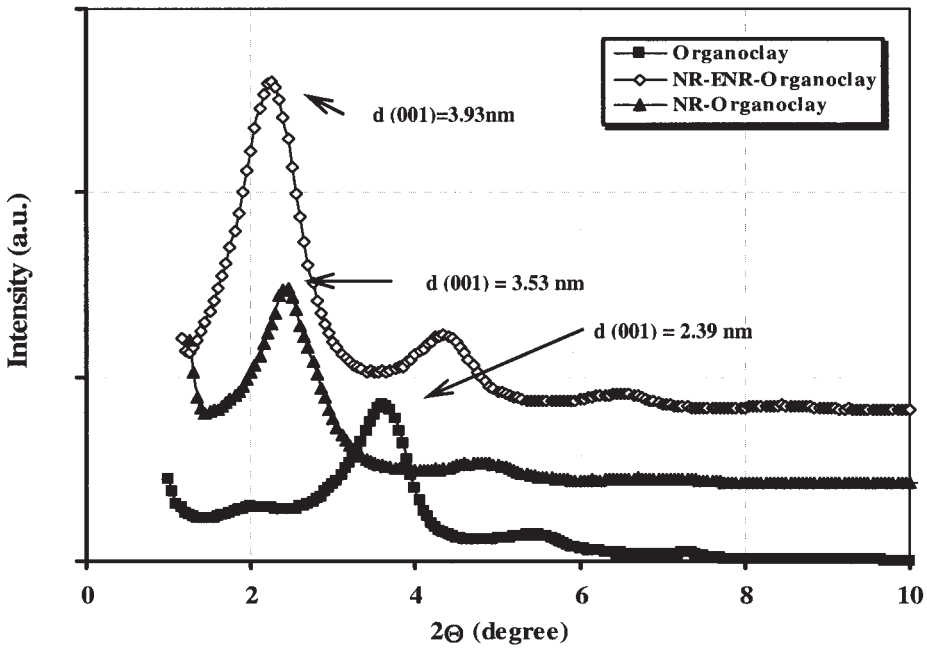

Figure 9 XRD spectra of the organoclay, NR/ENR 50/organoclay, and NR/organoclay nanocomposites filled with 10 phr organoclay.

best proof for the morphology dependent reinforcement in polymers. However, below the glass transition region, the effect of organoclay is not that significant.[30] The increase in the stiffness (modulus) is attributed to the presence of the clay particles in the nanocomposites. The significant enhancement found should be related to intercalation or exfoliation of the clay layers by the polymer chains. As a consequence, the high aspect ratio of the individual clay platelets becomes effective.

Figure 8(b) displays the mechanical loss factor (tan δ) as a function of temperature for the gum and 10 phr organoclay filled nanocomposite, respectively. The tan δ represented the ratio of dissipated energy to the stored energy and is related to the glass transition temperature of the polymer.[31] The reduction in the value of tan δ at T_g with the incorporation of 10 phr organoclay (filled) indicates a strong interaction between the rubber matrix and clay.[32] A secondary relaxation peak was also observed in the tan δ vs. T curve. This may represent the part of the rubber that is intercalated, i.e., located between the clay layers, as argued recently.[33]

X-ray diffraction

Figure 9 exhibits the XRD pattern of the organoclay, ENR 50 compatibilized NR, and NR nanocomposites and both filled with 10 phr of organoclay. The diffraction peak of the organoclay in the NR/ENR 50/organoclay nanocomposite shifted to a lower angle compared with the organoclay powder (from $2\theta = 3.7°$ to $2\theta = 2.25°$). This indicates that the d-spacing of the 001 peak shifted from the initial 2.39 nm to 3.93 nm. The d-spacing of the clay in the NR/organoclay nanocomposite also shifted from 2.39 to 3.53 nm (corresponding to a shift in 2θ from 3.7° to 2.5°). This implies that the rubber chains penetrated in between the clay layers in these two nanocomposites and thus produced an intercalated structure. So, the polymer/clay interaction seems to be able to overcome the van der Waals forces in between the interlayer.[34]

However, it is interesting to note that the d-spacing of the organoclay in the NR/ENR 50/organoclay nanocomposite is 11.3% higher than in the noncompatibilized NR/organoclay system. This indicates that the intercalation of the clay layers can be further improved when ENR 50 is added as compatibilizer.[23] The occurrence of eventual exfoliation in NR/ENR 50/organoclay nanocomposites was analyzed by TEM.

Transmission electron microscopy

Figure 10(a) shows a characteristic TEM image of NR/ENR 50/organoclay nanocomposite containing 2 phr organoclay. The dark lines in this figure correspond to the silicate layers that are evenly dispersed in the rubber matrix. It can be seen that the organoclay is being intercalated (agglomerates, tactoids) and exfoliated (individual layers) in the NR matrix. Similar morphological structures were also observed in works by McNally et al.[35] and Wang et al.[36] Based on Figure 10(b), showing a TEM picture of NR/ENR 50/organo-

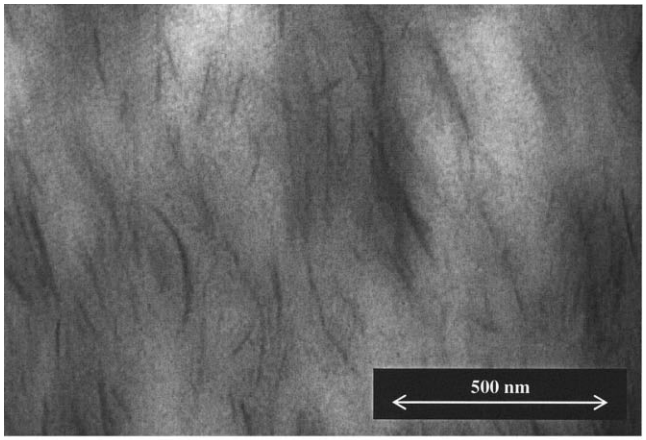

(a)

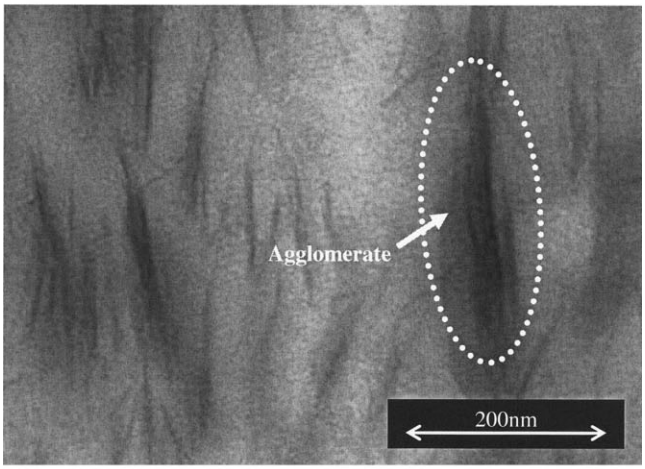

(b)

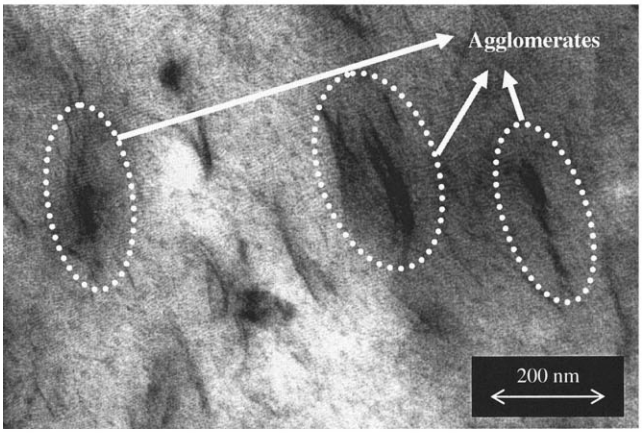

(c)

Figure 10 TEM micrograph of an NR/ENR 50/organoclay nanocomposite filled with (a) 2 phr organoclay, (b) 10 phr organoclay, and (c) TEM micrograph of NR/organoclay nanocomposite filled with 2 phr organoclay

clay filled with 10 phr organoclay, partial agglomeration (as labeled) can be revealed. It may be attributed to the poor interaction between NR and MMT.[37] This is in agreement with the observed deterioration in the mechanical properties at 10 phr filler loading.

The TEM images of NR/organoclay nanocomposite filled with 2 phr organoclay is shown in Figure 10(c). It provides a direct evidence for the poor dispersion of the organoclay in the NR matrix owing to which relatively low mechanical properties were measured (cf. Table II).

CONCLUSIONS

According to this study, scorch time and cure time decrease with increasing organoclay content, which is due to the presence of amine functional groups in the organoclay. The increment in maximum torque, minimum torque, and torque difference increase with increasing filler content indicates the enhancement of stiffness of the nanocomposite.

The addition of organoclay to NR improved the tensile and tear properties at optimum level, 2 phr filler content. This has been attributed to the better interfacial bonding between filler and the rubber matrix. It is interesting to note that the elongation at break still remained relatively high in comparison with gum compound. Organoclay decreased the compression set properties. As expected, the incorporation of organoclay increased the modulus and hardness, which is the measurement of the stiffness of the nanocomposites.

The result from DMTA explained the T_g relaxation and the elastic response to the deformation of the compound. XRD results indicated that nanocomposites are being intercalated into the MMT due to the expansion of *d*-spacing. TEM results showed that the MMT were intercalated and exfoliated at 2 phr of filler content. At 10 phr of organoclay, the MMT were partly exfoliated and partly reaggregated.

Addition of 10 phr of ENR 50 as the compatibilizer into the nanocomposites has not only resulted in faster curing but also a significant improvement of mechanical performance. This has been attributed to the better dispersion of MMT in nanocomposite as observed from XRD and TEM.

Thanks are due to Dr. Abu Amu (Head of Dry Rubber Unit, Malaysia Rubber Board) and Dr. A. A. Apostolov (University of Sofia, Bulgaria) for providing the compounding facilities, and performing the XRD measurements, respectively. We also thank Dr. R. Thomann (Freiburg, Germany) for performing the TEM measurements. Special scholarship granted by Universiti Sains Malaysia to one of us (Ms. T. P. Leng) is gratefully acknowledged.

References

1. Gloaguen, J. M.; Lefebvre, J. M. Polymer 2001, 42, 5841.
2. Vu, Y. T.; Mark, J. E.; Pham, L. H.; Engelhardt, M. J Appl Polym Sci 2001, 82, 1391.

3. Fornes, T. D.; Yoon, P. J.; Keskkula, H.; Paul, D. R. Polymer 2001, 42, 9929.
4. Liu, T. X.; Liu, Z. H.; Ma, K. X.; Shen, L.; Zeng, K. Y.; He, C. B. Compos Sci Technol 2003, 63, 331.
5. Kawasumi, M.; Hasegawa, N.; Kato, M.; Usuki, A.; Okada, A. Macromolecules 1997, 30, 6333.
6. Lee, J. W.; Lim, Y. T.; Park, O. O. Polym Bull 2000, 45, 191.
7. Hwu, J. M.; Jiang, G. J.; Gao, Z. M.; Xie, W.; Pan, W. P. J Appl Polym Sci 2002, 83, 1702.
8. Fan, J.; Liu, S.; Chen, G. M.; Qi, Z. N. J Appl Polym Sci 2002, 83, 66.
9. Chen, J. S.; Poliks, M. D.; Ober, C. K.; Zhang, Y.; Wiesner, U.; Giannelis, E. Polymer 2002, 43, 4895.
10. Xu, W. B.; Bao, S. P.; He, P. S. J Appl Polym Sci 2002, 84, 842.
11. Takeichi, T.; Zeidam, R.; Agag, T. Polymer 2002, 43, 45.
12. Hoffmann, B.; Kressler, J.; Stöppelmann, G.; Friedrich, C.; Kim, G. Colloid Polym Sci 2000, 278, 629.
13. Mousa, A.; Karger-Kocsis, J. Macromol Mater Eng 2001, 286, 260.
14. Nah, C.; Ryu, H. J.; Han, S. H.; Rhee, J. M.; Lee, M. H. Polym Int 2001, 50, 1265.
15. Liu, X.; Wu, Q. Polymer 2001, 42, 10013.
16. Callister, W. D. Materials Science and Engineering: An Introduction, 4th ed.; John Wiley & Sons: New York, 1997.
17. Blow, C. M. Rubber Technology and Manufacture, Institution of the Rubber Industry; Butterworths: London, 1971.
18. Sezna, J. A.; Pawlowski, H. A.; DeConinck, D. Proceeding of 136th Meeting of the ACS-Rubber Division, Fall, 1989.
19. Ismail, H.; Freakley, P. K. Eur Polym Mater 1996, 321, 411.
20. Poh, B. T.; Ismail, H.; Quah, E. H.; Chin, P. L. J Appl Polym Sci 2001, 81, 47.
21. Wu, Q.; Liu, X.; Berglund, L. A. Polymer 2002, 43, 2445.
22. Ishiaku, U. S.; Chong, C. S.; Ismail, H. Polym Test 2000, 19, 507.
23. Chang, Y.; Yang, Y.; Ryu, S.; Nah, C. Polym Int 2002, 51, 319.
24. Manna, A. K.; Tripathy, D. K.; De, P. P.; De, S. K.; Chatterjee, M. K.; Peiffer, D. G. J Appl Polym Sci 1999, 72, 1895.
25. Brown, R. P.; Soulagnet, G. Polym Test 2001, 20, 295.
26. Smith, L. P. The Language of Rubber; Butterworth Heinemann: London, 1993.
27. Othman, A. B. Polym Test 2001, 20, 159.
28. Hao, P. T.; Ismail, H.; Hashim, A. S. Paper presented at the 3rd Regional IMT–GT Ininet Conference, Medan, Indonesia, 2000.
29. Siriwardena, S.; Ismail, H.; Ishiaku, U. S. Polym Int 2001, 50, 707.
30. Varghese, S.; Karger-Kocsis, J.; Gatos, K. G. Polymer 2003, 44, 3977.
31. Alexandre, M.; Dubois, P. Mater Sci Eng R 2000, 28, 1.
32. Wan, C.; Qiao, X.; Zhang, Y. Polym Test 2003, 22, 453.
33. Varghese, S.; Karger-Kocsis, J. J Appl Polym Sci 2003, 44, 4921.
34. Kemp, W. Organic Spectroscopy; Macmillan Press: London, 1975.
35. McNally, T.; Murphy, W. R.; Lew, C. Y.; Turner, R. J.; Brennan, G. P. Polymer 2003, 44, 2761.
36. Wang, S.; Hu, Y.; Wang, Z.; Yong, T.; Chen, Z.; Fan, W. Polym Degrad Stab 2003, 80, 157.
37. Akkapeddi, M. K.; Morristown, H. Polym Compos 2000, 21, 576.